Immunology Letters 165 (2015) 90–101

Contents lists available at ScienceDirect

Immunology Letters

journal homepage: www.elsevier.com/locate/immlet

The mannose-6-phosphate analogue, PXS64, inhibits fibrosis *via* TGF-β1 pathway in human lung fibroblasts

Heidi Schilter[a,*], Carmen Z. Cantemir-Stone[b], Vladimir Leksa[c,d], Anna Ohradanova-Repic[c], Alison D. Findlay[a], Mandar Deodhar[a], Hannes Stockinger[c], Xiaomin Song[e], Mark Molloy[e], Clay B. Marsh[b], Wolfgang Jarolimek[a,f]

[a] *Drug Discovery, Pharmaxis, Australia*
[b] *Division of Pulmonary, Allergy, Critical Care, and Sleep Medicine, Department of Internal Medicine, Dorothy M. Davis Heart and Lung Research Institute, The Ohio State University, USA*
[c] *Molecular Immunology Unit, Institute for Hygiene and Applied Immunology, Center for Pathophysiology, Infectiology and Immunology, Medical University of Vienna, Austria*
[d] *Institute of Molecular Biology, Slovak Academy of Sciences, Slovak Republic*
[e] *Australian Proteome Analysis Facility, Macquarie University, Australia*
[f] *School of Medical & Molecular Biosciences, University of Technology Sydney, Australia*

ARTICLE INFO

Article history:
Received 10 April 2015
Accepted 14 April 2015
Available online 27 April 2015

Keywords:
PXS64
Mannose-6-phosphate
TGF-β1
M6P
Fibroblasts
Idiopathic pulmonary fibrosis

ABSTRACT

Idiopathic pulmonary fibrosis (IPF) is a chronic disease characterised by a progressive decline in lung function which can be attributed to excessive scarring, inflammation and airway remodelling. Mannose-6-phosphate (M6P) is a strong inhibitor of fibrosis and its administration has been associated with beneficial effects in tendon repair surgery as well as nerve repair after injury. Given this promising therapeutic approach we developed an improved analogue of M6P, namely PXS64, and explored its anti-fibrotic effects *in vitro*. Normal human lung fibroblasts (NHLF) and human lung fibroblast 19 cells (HF19) were exposed to active recombinant human TGF-β1 to induce increases in fibrotic markers. rhTGF-β1 increased constitutive protein levels of fibronectin and collagen in the NHLF cells, whereas HF19 cells showed increased levels of fibronectin, collagen as well as αSMA (alpha smooth muscle actin). PXS64 demonstrated a robust inhibitory effect on all proteins analysed. IPF patient fibroblasts treated with PXS64 presented an improved phenotype in terms of their morphological appearance, as well as a decrease in fibrotic markers (collagen, CTGF, TGF-β3, tenascin C, αSMA and THBS1). To explore the cell signalling pathways involved in the anti-fibrotic effects of PXS64, proteomics analysis with iTRAQ labelling was performed and the data demonstrated a specific antagonistic effect on the TGF-β1 pathway. This study shows that PXS64 effectively inhibits the production of extracellular matrix, as well as myofibroblast differentiation during fibrosis. These results suggest that PXS64 influences tissue remodelling by inhibiting TGF-β1 signalling in NHLF and HF19 cell lines, as well as in IPF patient fibroblasts. Thus PXS64 is a potential candidate for preclinical application in pulmonary fibrosis.

1. Introduction

Idiopathic pulmonary fibrosis (IPF) is a progressive and irreversible lung disease characterised by extensive scarring, inflammation and airway remodelling which results in marked distortion of lung architecture and the loss of respiratory function. Although the molecular mechanisms underlying IPF are largely unknown, it is proposed that the disease likely results from uncontrolled wound healing due to lung injury. A process, that if not reversed, can lead to aberrant proliferation of fibroblasts and excessive deposition of extracellular matrix (ECM).

Fibroblasts are an abundant cell type in the lung and play a central role in the maintenance of normal tissue function and structural integrity through controlled wound healing, proliferation and extracellular matrix production [1,2]. However, during fibrosis, they assume a migratory, proliferative, and ultimately a profibrotic, myofibroblastic phenotype [3]. Airway fibroblasts have the potential to synthesise and release latent TGF-β (LTGF-β) [4,5], which requires activation before it binds to its cognate receptor to exert

* Corresponding author at: Pharmaxis, 20 Rodborough Road, Frenchs Forest, 2086 NSW, Australia. Tel.: +61 2 94547283.
E-mail address: heidi.schilter@pharmaxis.com.au (H. Schilter).

http://dx.doi.org/10.1016/j.imlet.2015.04.003

its biological effect. Active TGF-β is often overexpressed in disease states [6–10] and its excessive production and activation enhances fibrosis progression by modulating fibroblast growth, migration and transformation [11–16].

Unfortunately currently available pharmacological interventions are unable to reverse disease pathogenesis during fibrosis. A potential therapeutic approach is the use of the phosphosugar mannose-6-phosphate (M6P) (Fig. 1, A), as it has been shown to be a strong inhibitor of fibrosis in a variety of animal models. Specifically, M6P possesses regenerative effects in flexor tendons during repair surgery [17–19] and enhances nerve repair during injury [20–22]. Early research with a M6P formulation accelerated re-epithelialisation, reduced redness and improved overall skin appearance (Renovo Group plc). Recently Adaprev treatment, a hypertonic solution containing M6P, was shown to reduce adhesions and improve collagen organisation following tendon injury *in vivo* [23]. Interestingly, the action of M6P is not specific to fibrosis, as this treatment also conferred protection against experimental autoimmune encephalomyelitis (EAE) [24], arthritis [25] and peritonitis [26]. In addition, M6P inhibited thyroid allograft rejection by reducing leukocyte infiltration into the grafts [26].

Based on these promising applications, we sought to develop an improved analogue of M6P, namely PXS25 (Fig. 1, B), with increased chemical and metabolic stability. Its efficacy was tested in the fibrotic diabetic nephropathy *in vitro* model [27]. Upon PXS25 exposure, the secretion of matrix proteins was significantly dampened [27]. Despite these encouraging preliminary results, the highly hydrophilic nature of PXS25 conferred low cell permeability and limited bioavailability following oral administration. To overcome this issue and improve the physicochemical properties of PXS25, a lipophilic prodrug (namely PXS64, Fig. 1C), was synthesised. Due to its characteristics, PXS64 is able to quickly diffuse across membranes and be hydrolysed into PXS25.

The present study shows that the mannose-6-phosphate analogue PXS64 effectively inhibited the production of ECM proteins, as well as myofibroblast differentiation during TGF-β1-driven fibrosis. Mechanistic studies using proteomics with iTRAQ labelling and mass spectrometry quantitation indicate a specific antagonistic effect of PXS64 on the TGF-β1 pathway. These results identify PXS64 as a potential candidate for clinical application to reduce ECM deposition in pulmonary fibrosis.

2. Methods

2.1. Compound chemical properties

Replacement of the hydrolytically labile phosphate moiety of mannose-6-phosphate with a phosphonate bioisostere, as well as introduction of a lipophilic group at the anomeric position, led to the development of PXS25. Further derivatisation of PXS25, *via* preparation of the corresponding bis(pivaloyloxymethyl) ester [bis(POM) ester] then provided PXS64. This modification was made so as to increase the associated clogP value of PXS64 (relative to PXS25) and thus improve the physicochemical profile of the compound.

2.2. Cell culture

2.2.1. Culture

NHLF cells are a human primary lung fibroblast cell line purchased from Lonza. NHLF were maintained in Lonza custom FBM-2 media (fibroblast basal media) with additional Lonza SingleQuots supplements (FGM-2) containing insulin, recombinant GFG-B, GA-1000 and FBS and incubated at 37 °C with 5% CO_2.

HF19 is an immortalised human lung fibroblast cell line and was purchased from Cell Bank, Australia. HF19 fibroblasts were maintained in MEM media (In Vitro Technologies) containing penicillin G, streptomycin (50 units/mL and 50 μg/mL respectively), L-glutamine (2 mM), 10% heat-inactivated foetal calf serum (FCS) and non-essential amino acids (100 μM) and incubated at 37 °C with 5% CO_2.

Primary lung fibroblasts from normal (CCL-201; CCL-204) and IPF patients (CCL-134; CCL-191) were purchased from and cultured as recommended by ATCC. Cell cultures were used within passage 6. The IPF cells originate from young IPF patients and have been published previously [28].

Human CIMPR-positive mouse fibroblasts were generated from CIMPR-negative mouse fibroblasts [29] through the retroviral expression system as described elsewhere [30]. Mouse fibroblasts were cultured in RPMI 1640 medium supplemented with penicillin, streptomycin, glutamine, and 10% fetal calf serum under standard conditions.

2.2.2. Cell density

Cells were seeded into 6-well plates at 1×10^5/well and 2×10^5/well to reach subconfluence and overconfluence, respectively.

2.2.3. Experimental procedure

The day prior to experiment, fibroblasts were starved in 0.1% FCS (starving media) and corresponding supplements. In a pilot study rhTGF-β1 was tested in the HF19 cells at different concentrations: 1, 2 and 10 ng/mL (e-biosciences). While 1 ng/mL was not effective, 2 and 10 ng/mL induced comparable effects. In following experiments rhTGF-β1 was used at 2 ng/mL. Pirfenidone (Sigma) was used at 50 μg/mL.

For pre-, co- and post-incubation experimental setups, compounds were added to the cell culture as indicated in Section 3.

2.3. Protein extraction and Western blot analysis

Fibroblasts were washed twice with PBS, scraped and lysed in cell lysis buffer containing 20 mM Tris, 150 mM NaCl chloride, 50 mM NaF, 1 mM EDTA and 1% Triton, 1× Complete© protease inhibitor and 1× protease inhibitors. The samples were stored at −20 °C until analysis. Total protein was determined using Quant-iT assay (Invitrogen) as per the manufacturer's instructions. All cell lysates were adjusted to equal total protein levels. The samples (45 μL) were mixed with sample buffer (15 μL) containing 10 mM β-mercaptoethanol, heated to 100 °C for 5 min, and separated by 10% Bis–Tris or 4–12% Bis–Tris NuPAGE gel (Invitrogen) using MOPS buffer. Gels were transferred to PVDF membranes for blotting. Afterwards, the membranes were incubated with primary antibody: polyclonal anti-human αSMA (Abcam, 1:400), polyclonal anti-human collagen (Abcam, 1:1000), polyclonal anti-human fibronectin (Abnova, 1:1000) or polyclonal anti-mouse Tubulin (Sigma, 1:2000) in 1% BSA in PBS–Tween (0.1%) overnight. The membrane was then washed three times with PBS–Tween (0.1%) using Millipore SNAP i.d. vacuum and incubated with corresponding secondary antibodies conjugated to horseradish peroxidase (HRP) 1:1000. The fusion system was used to acquire membrane chemiluminescence, and signals were analysed by Image J against the tubulin control.

2.4. RNA isolation and real-time PCR analysis

IPF cells. Total RNA was isolated using Trizol (Invitrogen). DNAs were removed using Turbo DNA-free kit (Ambion). RNA was subjected to cDNA synthesis (Invitrogen) and quantitative real-time

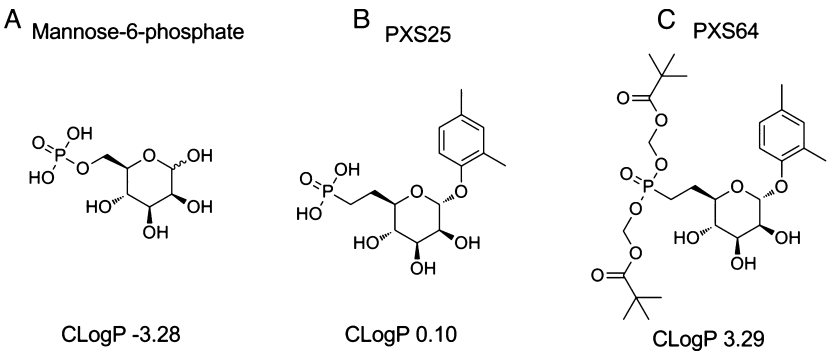

Fig. 1. Chemical structures of M6P and analogues. Structures of (A) mannose-6-phosphate; (B) PXS25 and (C) PXS64. The calculated log P (clogP) values were derived using ChemDraw Ultra, version 12.

(qRT)–PCR using SYBR Green Master Mix. Quantitative gene expression was performed using 50 ng complementary DNA per reaction. Primers to measure gene expression were purchased from IDT. Reactions were performed on the ABI 7900HT real-time PCR System (Applied Biosystems) at the Davis Heart and Lung Research Institute, Ohio State University (Columbus, OH). A list of quantitative RT-PCR primers can be found below. GAPDH was used as the reference gene.

CIMPR cells. Total RNA was extracted with the PureLink RNA Mini Kit according to the manufacturer's instructions (Ambion), followed by the cDNA synthesis using SuperScript VILO cDNA Synthesis Kit (Invitrogen). Gene expression was measured by the 2-ΔΔCT method based on quantitative real-time PCR using CFX96 Real-Time PCR system (Bio-Rad) with the ABI TaqMan primer sets for mouse GAPDH and fibronectin specified below. Results are reported relative to the values for DMSO-treated CIMPR−/− cells, which were set to 1.

GENE	Sequence	
Collagen 1a1	5′-CCCCTGGAAAGAATGGAGATG-3′	Forward
	5′-TCCAAACCACTGAAACCTCTG-3′	Reverse
Connective Tissue Growth Factor	5′-ACCAATGACAACGCCTCC-3′	Forward
	5′-TTGGAGATTTTGGGAGTACGG-3′	Reverse
Transforming Growth Factor 3	5′-AGTGGCTGTCCTTTGATGTC-3′	Forward
	5′-CACCTCGTGAATGTTTTCCAG-3′	Reverse
TENASCIN C	5′-CACTACACAGCCAAGATCCAG-3′	Forward
	5′-TCGTGTCTCCATTCAGCATTG-3′	Reverse
Fifbronectin	5′-ACTGTACATGCTTCGGTCAG-3′	Forward
	5′-AGTCTCTGAATCCTGGCATTG-3′	Reverse
Smooth Muscle Actin (alpha)	5′-AGGAGTGGTTGCTGAATGAG-3′	Forward
	5′-GTCTCATAGTCCTTCTGTCGC-3′	Reverse
Thrombospondin1	5′-CTCCCCTATGCTATCACAACG-3′	Forward
	5′-AGGAACTGTGGCATTGGAG-3′	Reverse
Glyceraldehyde-3-phosphate dehydrogenase	5′-ACATCGCTCAGACACCATG-3′	Forward
	5′-TGTAGTTGAGGTCAATGAAGGG-3′	Reverse

GENE	ABI taqman probe
Fibronectin	Mm 01256744-m1
Glyceraldehyde-3-phosphate dehydrogenase	4352932E

2.5. Sample preparation for proteomic analysis

Fibroblasts were plated at 80% density and incubated with 10 μM of PXS64 30 min prior to the addition of rhTGF-β1 (2 ng/mL). After 4 h, fibroblasts were washed gently twice with phosphate-buffered saline (PBS), before replacing with fresh starve media and incubating for a further 20 h.

At harvest, crude cellular protein extracts were obtained by lysing fibroblasts in a buffer containing 20 mM HEPES-NaOH (pH8.0), 150 mM NaCl, 50 mM NaF, 1 mM EDTA, 1% SDS with 1x Complete© protease and phosphatase inhibitors. Samples were then subjected to trichloroacetic acid (TCA)/acetone precipitation. A fresh TCA solution was prepared before the extraction process. Solutions were mixed in a 1:8:1 ratio in the following order: 1 mL cell lysate + 8 mL 100% ice-cold acetone + 1 mL 100% TCA and precipitated at −20 °C for 1 h. Samples were then centrifuged at 18,000 × *g* for 15 min at 4 °C. Supernatant was discarded and pellets were washed with 1 mL ice-cold acetone and re-centrifuged at 18,000 × *g* for 15 min at 4 °C. The pellet was dried at room temperature. 45 μg of each sample was reduced with TCEP, alkylated with MMTS and digested with trypsin. Samples were labelled using iTRAQ 4-plex reagents for 1 h following the manufacturer's instructions (ABSciex) and as previously described [31,32]. Samples were then combined at 1:1 ratios.

2.5.1. Strong cation exchange HPLC

The iTRAQ labelled peptides were fractionated by SCX HPLC using a PolyLC PolySulfoethyl A (200 mm × 2.1 mm × 5 μm, 200 Å) column. The buffer A was 5 mM phosphate 25% acetonitrile, pH 2.7 and buffer B was 5 mM phosphate 350 mM KCl 25% acetonitrile, pH 2.7. After sample loading and washing with buffer A, buffer B concentration increased from 10% to 45% in 70 min and then increased quickly to 100% for 10 min at a flow rate of 300 μl/min. The eluent from SCX was collected every ½ min at the beginning of the gradient and at 4 min intervals thereafter. SCX fractions were dried by vacuum centrifugation.

2.5.2. NanoLC ESI MS/MS data acquisition

The SCX fractions were resuspended in 40 μL of loading/desalting solution (0.1% trifluoroacetic acid and 2% acetonitrile 97.9% water). 39 μL of the resuspended solution was loaded on a reverse phase peptide Captrap (Michrom Bioresources) and desalted. After desalting, the trap was switched on line with a 150 μm × 10 m C18 3 μm 300A ProteCol column (SGE). The buffer solution A was 99.9% water/0.1% formic acid and buffer solution B was 90% acetonitrile/9.9% water/0.1% formic acid. The buffer B concentration was increased from 5% to 90% in 120 min in three linear gradient steps to elute peptides. After peptide elution, the column was cleaned with 100% B for 15 min and then equilibrated with buffer A for 30 min before the next sample injection. The reverse phase NanoLC eluent was subject to positive ion nanoflow electrospray analysis in an information dependant acquisition (IDA) mode using a QSTAR Elite mass spectrometer (AB Sciex). In IDA mode a TOFMS survey scan was acquired (*m*/*z* 370–1600, 0.5 s), with the three most intense multiply charged ions (counts >70) in the

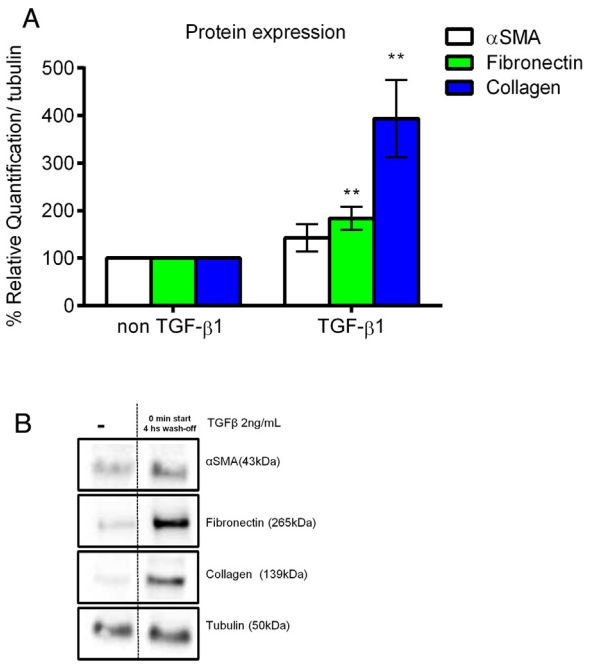

Fig. 2. Normal human lung fibroblast protein expression after rhTGF-β1 stimulation. rhTGF-β1 increased protein levels of fibronectin and collagen while the expression of αSMA (alpha smooth muscle actin) was not significantly increased. (A) Quantification was relative to tubulin and normalised as a % of the non-TGF-β1 group. (B) Representative blot of fibronectin, collagen and αSMA expression upon rhTGF-β1stimulation. Data presented are S.E.M. of ≥3 independent experiments using single cultured experiments. $^{**}p < 0.01$ compared to non-TGF-β1.

survey scan sequentially subjected to MS/MS analysis. MS/MS spectra were acquired in the mass range m/z 100–1600.

2.5.3. Data processing

The MS/MS data were submitted to ProteinPilot V4.0 (AB Sciex) for peptide identification and quantitation using Swiss-prot human database. Bias correction was selected to normalise iTRAQ intensities for each sample. False discovery rate analysis was enabled. After ProteinPilot data processing, protein and peptide summaries were exported as text files. Proteins with larger than 1.3 unused score (better than 95% confidence) were used for further protein quantitation statistical analysis.

2.6. Statistical analysis

Unless otherwise stated, data presented are mean ± S.E.M. of ≥3 independent experiments using single cultured experiments. A significant difference between control and multiple treatment groups was assessed by one-way ANOVA using Dunnett's *post hoc* test for multiple comparisons. Comparisons of two groups were performed by unpaired student's *t* test.

3. Results

3.1. rhTGF-β1 enhanced the expression of fibrotic makers in normal human lung fibroblasts

In response to active TGF-β1, lung fibroblasts undergo a phenotypic transformation which is associated with tissue remodelling, increased expression of collagen, fibronectin and α smooth muscle protein (αSMA) as well as increased proliferative state and nodule formation [34–38]. All of which can be replicated *in vitro* [33]. In the present study rhTGF-β1 was utilised *in vitro* to model changes associated with fibrosis in normal human lung fibroblasts

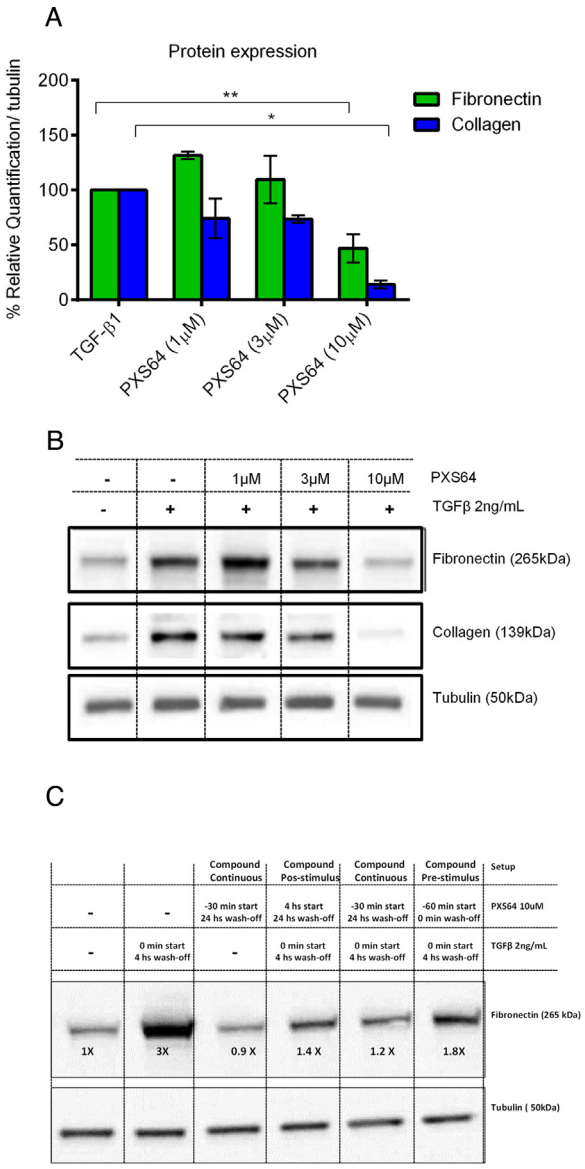

Fig. 3. Normal human lung fibroblast protein expression after PXS64 treatment. (A) NHLF cells were pre-treated with PXS64, followed by stimulation with rhTGF-β1. PXS64 at 10 μM demonstrated a robust inhibitory effect of fibronectin and collagen. Quantification was relative to tubulin and normalised as a % of the TGF-β1 group. (B) Representative blot of fibronectin and collagen increases upon rhTGF-β1stimulation and the dose dependent response of PXS64. (C) NHLF cells were treated with PXS64 at different times and stimulated with rhTGF-β1. Compound continuous occurred when fibroblasts were pre-equilibrated with PXS64 for 30 min and PXS64 maintained in culture until the end of the experiment (24 h). Pos-stimulus denominates when PXS64 was added to the fibroblasts after 4 h of rhTGF-β1 stimulation and maintained in culture until the end of the experiment (24 h). Pre-stimulus occurred when fibroblasts were exposed to PXS64 for 1 h, PXS64 was then removed and then stimulated to rhTGF-β1. PXS64 at 10 μM demonstrated a robust inhibitory effect of fibronectin protein expression independent of treatment time. Data presented are S.E.M. of ≥3 independent experiments using single cultured experiments. $^{**}p < 0.01$ $^{*}p < 0.05$ compared to TGF-β1.

(NHLFs). NHLFs were seeded at subconfluency (80%) and treated with 2 ng/mL of rhTGF-β1. Four hours after addition of the cytokine, the fibroblasts were gently washed and maintained in culture for 20 h.rhTGF-β1 increased protein levels of fibronectin and collagen (Fig. 2A/B) by two and four fold compared to unstimulated fibroblasts, respectively. The expression of αSMA was not significantly increased (Fig. 2A/B); as such this marker was not further evaluated in this cell line.

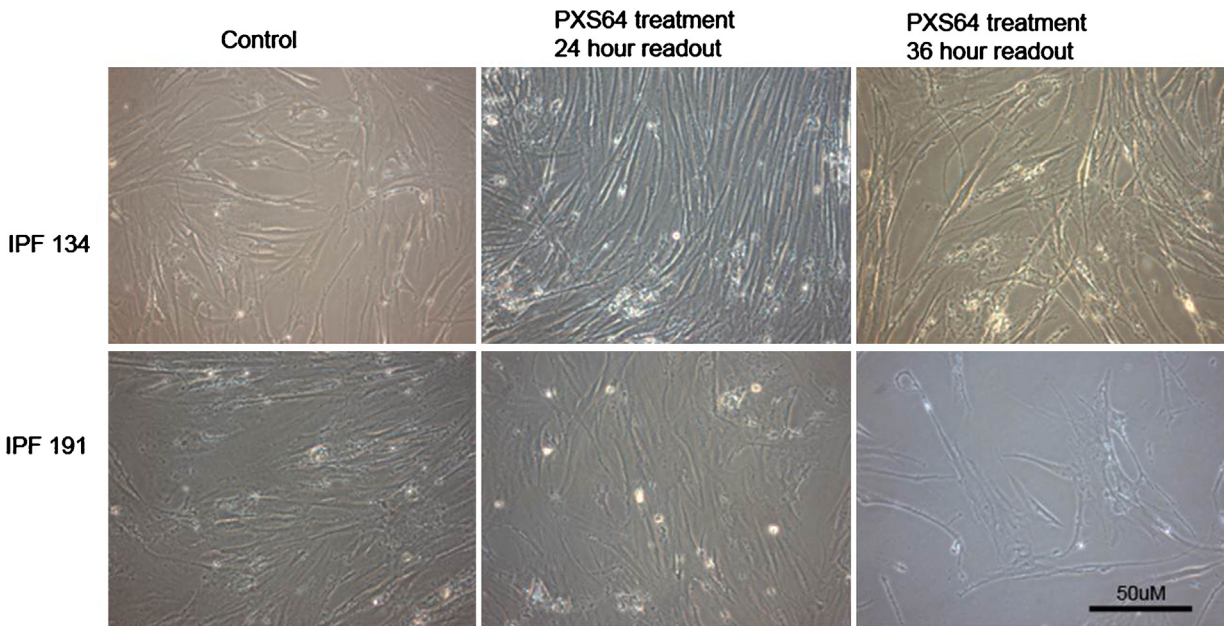

Fig. 4. Idiopathic pulmonary fibrosis patient fibroblasts after PXS64 treatment.
IPF patient fibroblasts (IPF 134, IPF 191 from Lonza) were treated with 10 μM of PXS64 for 24 h. Cellular morphology was assessed at 24 and 36-h time points. The fibroblasts presented an improved phenotype in terms of their morphological appearance after 24 h of PXS64 treatment. This effect was sustained even at the 36-h time point, when PXS64 was no longer present in the medium.

These initial studies established that active recombinant TGF-β1 at 2 ng/mL for a pulse of 4 h caused maximal stimulation and therefore this protocol was utilised in further studies.

3.2. Effects of PXS64 on rhTGF-β1 stimulated NHLFs

Based on previous studies by Wong et al. [27], in which the M6P analogue PXS25 was shown to effectively inhibit fibrosis, it was hypothesised that PXS64 would also have the capacity to decrease rhTGF-β1 fibrotic effects on NHLFs.

NHLF cells were pre-equilibrated with PXS64 for 30 min prior to the addition of rhTGF-β1. After 4 h, rhTGF-β1 was removed and fibroblasts were maintained in medium containing PXS64; the cells were then incubated for the next 20 h. PXS64 demonstrated a significant inhibition of fibrotic markers, with the highest efficacy observed at 10 μM (Fig. 3A/B); at this concentration it supressed fibronectin expression by 53% ± 12% (SEM) $^{**}p < 0.01$ and of collagen by 86% ± 3% (SEM) $^{*}p < 0.05$ (Fig. 3A/B). PXS64 exhibited a steep dose response curve in reducing fibrotic gene expression with the optimal concentration at 10 μM. Given the prominent and consistent inhibitory effect associated with 10 μM of PXS64, this dose was selected for subsequent mechanistic studies.

In order to determine whether continuous treatment of fibroblasts with PXS64 was necessary for its anti-fibrotic effect, the fibroblasts were exposed to PXS64 for only 60 min prior to rhTGF-β1 stimulation. Interestingly, with only a brief pulse followed by two washes to remove the compound from the supernatant, PXS64 demonstrated a robust inhibitory effect of fibronectin (Fig. 3C, compound pre-stimulus) thus indicating a lasting effect mediated only by a transitory exposure to the compound.

In previous experiments, PXS64 was administered prior to cytokine stimulation. To rule out the possibility that PXS64 somehow inhibited cell priming (*i.e.* blocking active TGF-β1 internalisation, thus preventing cell activation) fibroblasts were pulsed with PXS64 after 4 h of rhTGF-β1 addition. In this instance, the treatment was found to reverse the effects of rhTGF-β1 on fibronectin (Fig. 3C, compound post-stimulus), indicating that PXS64 does not impede cell activation or priming, but rather reduces TGF-β1 downstream signalling.

3.3. Effects of PXS64 on idiopathic pulmonary fibrosis patient lung fibroblasts

To relate the effects of PXS64 to human disease, human lung fibroblasts from IPF patients were next cultured. IPF fibroblasts have altered expression in ubiquitination-mediators, proteasomal constituents, Wnt signalling, apoptosis, metabolic pathways and cell cycle regulators. Although IPF cells can be stimulated by rhTGF-β1, they constitutively produce a plethora of cytokines and growth factors and thus do not require exogenous rhTGF-β1 stimulation to activate fibrotic markers [39,40]. The fibroblasts were treated with 10 μM of PXS64 for 24 h and fibrotic markers were analysed at either the 24 or 36-h time points.

After 24 h, the fibroblasts presented an improved phenotype in terms of their morphological appearance. In the presence of PXS64 they changed from a senescent, growth-arrested state (as expected to be seen in IPF fibroblasts) to a regular fusiform, healthy phenotype (Fig. 4). Even when fibroblasts were no longer in contact with the compound (36-h time point, 12 h without PXS64) anti-fibrotic effects were still observable, suggesting that the cells did not require continuous exposure to PXS64 (Fig. 4). mRNA analysis of IPF cells demonstrated that a number of fibrotic associated genes, such as collagen, connective tissue growth factor (CTGF), TGF-β3, tenascin C, αSMA and thrombospondin 1 (THBS1), were down-regulated by PXS64 treatment (Table 1). Importantly, fibrotic mRNA expression was further decreased after 36 h, *i.e.* even when the fibroblasts were no longer in contact with PXS64. This suggested a long lasting inhibitory effect of PXS64 on these cells. Furthermore, collagen, TGF-β3, tenascin C and fibronectin inhibition were actually greater at the 36-h time point, providing further support of the anti-fibrotic efficacy of PXS64.

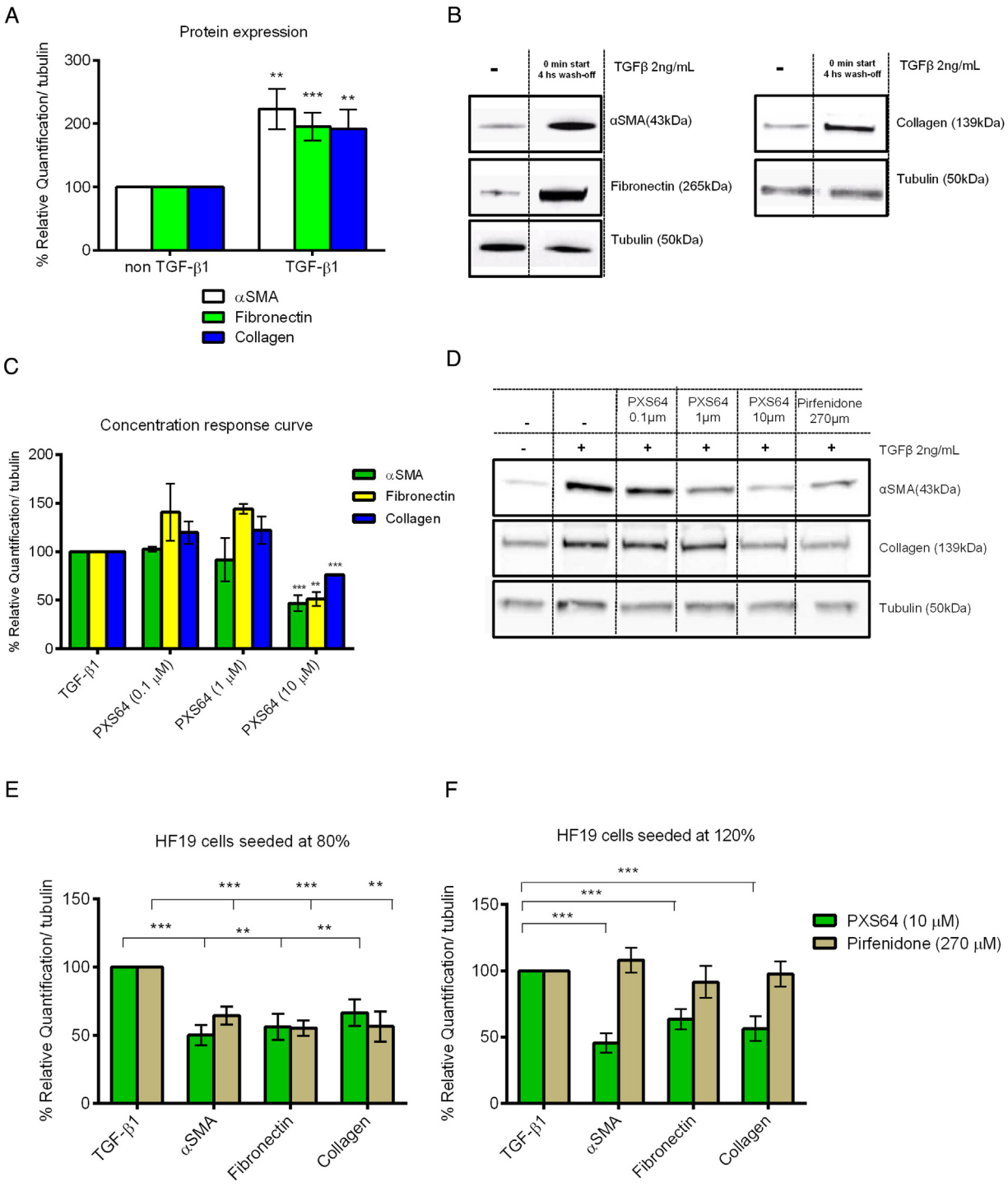

Fig. 5. H19 (human lung fibroblast) protein expression after rhTGF-β1 and PXS64 treatment. (A) HF19 cells were treated with rhTGF-β1 and cells showed increased protein levels of αSMA (alpha smooth muscle actin), fibronectin, and collagen. Quantification was relative to tubulin and normalised as a % of the non-TGF-β1 group ***$p < 0.01$ **$p < 0.01$ compared to non-TGF-β1 group. (B) Representative blot of αSMA, fibronectin and collagen increases upon rhTGF-β1stimulation. (C) HF19 cells were pre-treated with PXS64, followed by stimulation with rhTGF-β1. PXS64 at 10 μM demonstrated a robust inhibitory effect of all proteins tested. Quantification was relative to tubulin and normalised as a % of the TGF-β1 group. (D) Representative blot of αSMA and collagen increases upon rhTGF-β1stimulation and dose dependent response of PXS64. (E) HF19 cells were seeded at 80% confluency and treated with PXS64 or Pirfenidone, PXS64 exhibited a very potent anti-fibrotic activity comparable to the effect mediated by Pirfenidone. (F) HF19 cells were seeded at 120% density, PXS64 still displayed inhibitory properties, in contrast to the lack of effect displayed by Pirfenidone. Quantification was relative to tubulin and normalised as a % of TGF-β1 group ***$p < 0.01$ **$p < 0.01$ compared to the TGF-β1 group. All data presented are S.E.M. of ≥3 independent experiments using single cultures.

3.4. *Effects of PXS64 on cell density*

A number of studies have suggested that cell density influences cell behaviour upon stimulation [41–45], as such the action of PXS64 was tested in a high density environment by seeding fibroblasts at 120% confluency. However, normal human lung fibroblasts did not proliferate under these conditions. Further studies were therefore performed on HF19 cells, an immortal human lung fibroblast line.

Table 1
Idiopathic pulmonary fibrosis patient fibroblasts after PXS64 treatment IPF patient fibroblasts were treated with 10 μM of PXS64 for 24 h. mRNA expression of fibrotic markers was assessed at 24 and 36-h time points. A number of fibrotic markers were down-regulated by PXS64 treatment. It was found that the expression was further decreased after 36 h, even when the fibroblasts were no longer in contact with PXS64. Data presented are from one experiment using single culture.

	Compared to IPF control	
	24 h Post PXS64	36 h Post PXS64
Collagen	−40%	−70%
Connective tissue growth factor	−45%	−52%
TGF-β3	−30%	−83%
Tenascin C	−11%	−42%
Fibronectin	+4%	−49%
αSMA	−82%	−51%
Thrombospondin 1	−69%	−43%

Firstly, HF19 cells were found to be sensitive to active rhTGF-β1 as the expression of fibrotic markers increased upon stimulus with rhTGF-β1 (Fig. 5A/B). In contrast to NHLFs, αSMA expression increased in HF19 after rhTGF-β1 treatment, indicating differences between the two cell types. In a similar manner to NHLFs, HF19 cells were treated with different doses of PXS64, and the effect at 10 μM was found to be maximal (Fig. 5C/D).

HF19 cells were then seeded at different confluences and were also treated with Pirfenidone, a small molecule with well documented anti-fibrotic activities. When fibroblasts were seeded at 80% confluency, PXS64 exhibited a very potent anti-fibrotic activity (as measured by the inhibition of αSMA, fibronectin and collagen) comparable to the effect mediated by Pirfenidone (Fig. 5D/E). Moreover, when the fibroblasts were seeded at overconfluency, PXS64 maintained inhibitory properties, in contrast to the lack of effect displayed by Pirfenidone (Fig. 5F).

3.5. *PXS64 acts independently of cation-independent mannose 6-phosphate receptor (CIMPR)*

Multiple reports have described the M6P dependent activation of latent TGF-β1 [46–48], which is thought to occur through the M6P-binding sites on CIMPR (cation-independent mannose 6-phosphate receptor) [48]. It was therefore anticipated that PXS64 could also inhibit TGF-β1 signalling through CIMPR as was also postulated for PXS25 [27]. As such, mouse CIMPR−/− fibroblasts (Fig. 6A) and mouse CIMPR−/− fibroblasts reconstituted with human CIMPR (Fig. 6B) were pre-treated with 10 μM of PXS25, PXS64 or mannose-6-phosphate (M6P) followed by 4 h incubation with rhTGF-β1. After rhTGF-β1 removal, fibroblasts were incubated with the corresponding inhibitor and analysis was performed at the 24-h time point. Interestingly, whilst neither PXS25 nor M6P showed any effects, PXS64 was found to reduce fibronectin levels in the CIMPR−/− fibroblasts (Fig. 6A), thereby suggesting a divergent mechanism by which PXS64 can exert ant fibrotic effects. To further explore this observation CIMPR−/− fibroblasts were reconstituted with human CIMPR (Fig. 6B). Once again either PXS25 or M6P did not inhibit rhTGF-β1-induced fibronectin expression in this fibroblast cell line. In contrast, PXS64 demonstrated a reduction in fibronectin. Similar results were obtained in immunoblotting analyses (data not shown).

Taken together these results show that PXS64 acts independently of CIMPR and that there are clear differences between the mechanism of action displayed by PXS64 when compared with PXS25 and M6P.

Table 2
Proteomics analysis of HF19 upon rhTGF-β1 stimulation Fibroblasts were treated with rhTGF-β1 for 4 h, and proteomics analysis was done at the 24-h time point. Protein values were calculated as a ratio between two groups of interest. To be regarded as significant, proteins were required to be a true value (as assessed by Ingenuity software) and considered highly regulated (≤0.83 for down-regulated proteins or ≥1.2 for up-regulated proteins). Upon rhTGF-β1 treatment, 55 proteins were differentially regulated in the HF19 cell line. The proteins highlighted by the asterisk are similarly regulated by rhTGF-β1 in the NHLF cells. Data presented are from two independent experiments using single cultures.

Name	TGF-β1 vs none
Thrombospondin-1 ***	2.24
Plasminogen activator inhibitor 1 ***	2.24
Elastin	2.17
Tensin-1 ***	2.03
Connective tissue growth factor	2.02
Cadherin-6	1.98
Fibronectin ***	1.89
Collagen alpha-1(IV) chain	1.83
Collagen alpha-1(V) chain	1.80
Palladin	1.72
Catenin beta-1	1.67
Procollagen-lysine,2-oxoglutarate 5-dioxygenase 2 ***	1.64
Tenascin ***	1.54
Collagen alpha-1(I) chain ***	1.53
Transforming growth factor-beta-induced protein ig-h3 ***	1.53
Inactive tyrosine-protein kinase 7	1.52
Asparagine synthetase [glutamine-hydrolyzing]	1.48
CTP synthase 1	1.48
Importin-7	1.47
Fermitin family homolog 2 ***	1.45
Transforming growth factor beta-1-induced transcript 1 protein	1.44
Plastin-3 ***	1.41
Caldesmon ***	1.41
Elongation factor 2	1.41
SPARC	1.41
Collagen alpha-2(I) chain ***	1.40
ATP-citrate synthase	1.39
PDZ and LIM domain protein 5	1.38
UDP-glucose 6-dehydrogenase	1.38
Catenin alpha-1 ***	1.34
Versican core protein	1.33
Prolyl 4-hydroxylase subunit alpha-2 ***	1.31
Four and a half LIM domains protein 2	1.31
Vigilin	1.30
Glucosamine--fructose-6-phosphate aminotransferase [isomerizing] 1 ***	1.30
PDZ and LIM domain protein 4	1.30
6-phosphofructokinase type C	1.30
General vesicular transport factor p115	1.29
Delta-1-pyrroline-5-carboxylate synthase	1.27
Cold shock domain-containing protein E1	1.25
Catenin delta-1	1.24
Protein transport protein Sec23A	1.20
Electron transfer flavoprotein subunit beta	0.83
Astrocytic phosphoprotein PEA-15	0.82
Myristoylated alanine-rich C-kinase substrate ***	0.80
Histone H1.5	0.80
NAD(P)H dehydrogenase [quinone] 1	0.78
Caveolin-1	0.78
CD166 antigen ***	0.76
Histone H4	0.74
High mobility group protein HMG-I/HMG-Y	0.73
Leukocyte surface antigen CD47	0.71
Stathmin	0.70
Nuclease-sensitive element-binding protein 1 ***	0.65
Insulin-like growth factor-binding protein 5	0.58

Low Signal High

3.6. *PXS64 is an antagonist on the TGF-β1 pathway*

To elucidate the underlying mechanism of PXS64 action, proteomic profiling of HF19 and NHLF cells was performed. The composition of the fibroblast proteome resulted in the identification of over 1200 proteins (FDR 0.1% by ProteinPilot FDR analysis

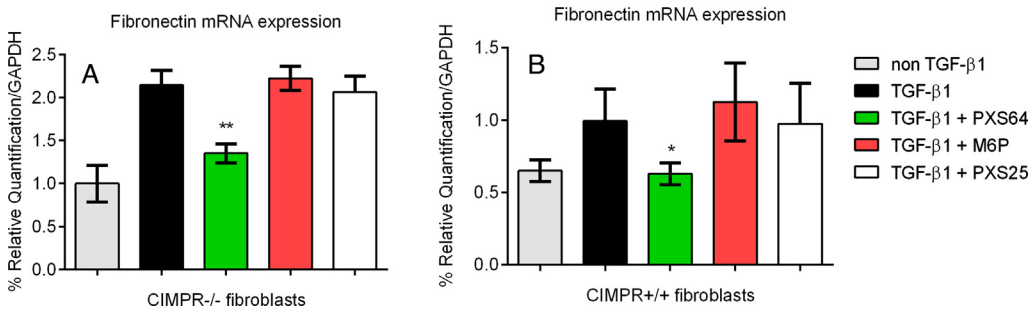

Fig. 6. CIMPR deficiency does not affect PXS64 treatment. Mouse fibroblasts were pre-treated with 10 μM of PXS25, PXS64 or mannose-6-phosphate (M6P), followed by rhTGF-β1 stimulation. The rhTGF-β1 induced increase of fibronectin was diminished by PXS64 in (A) CIMPR−/− fibroblasts as well as in (B) mouse CIMPR−/− fibroblasts reconstituted with human CIMPR. Data presented are S.E.M. of ≥2 independent experiments using single cultures. $^{**}p < 0.01$ $^{*}p < 0.05$ compared to the TGF-β1 group.

Table 3
Proteomics analysis of NHLF upon rhTGF-β1 stimulation Fibroblasts were treated with rhTGF-β1 for 4 h, and proteomics analysis was done at the 24-h time point. Protein values were calculated as a ratio between two groups of interest. To be regarded as significant, proteins were required to be a true value (as assessed by Ingenuity software) and considered highly regulated (≤0.83 for down-regulated proteins or ≥1.2 for up-regulated proteins). Upon rhTGF-β1 treatment, 82 proteins were differentially regulated in the NHLF cell line. The proteins highlighted by the asterisk are similarly regulated by rhTGF-β1 in the HF19 cells. Data presented are from one experiment using single culture.

Name	TGFB1 vs none
Collagen alpha-1(I) chain ***	3.28
Glia-derived nexin	3.07
Collagen alpha-2(I) chain ***	3.04
Plasminogen activator inhibitor 1 ***	2.99
Transforming growth factor-beta-induced protein ig-h3 ***	2.66
Tenascin ***	2.57
Fibronectin ***	2.42
Tensin-1 ***	2.03
Protein disulfide-isomerase	1.89
40S ribosomal protein S8	1.79
Procollagen-lysine,2-oxoglutarate 5-dioxygenase 2 ***	1.79
Inhibitor of nuclear factor kappa-B kinase-interacting protein	1.76
60S ribosomal protein L38	1.67
Alpha-actinin-1	1.66
Thrombospondin-1 ***	1.61
LIM and senescent cell antigen-like-containing domain protein 1	1.61
SPARC	1.60
Moesin	1.60
60S ribosomal protein L11	1.59
Probable ATP-dependent RNA helicase DDX17	1.58
26S proteasome non-ATPase regulatory subunit 12	1.55
Cytoplasmic FMR1-interacting protein 1	1.46
Prolyl 4-hydroxylase subunit alpha-2 ***	1.46
Transgelin	1.45
Peptidyl-prolyl cis-trans isomerase B	1.45
Nesprin-1	1.42
AP-2 complex subunit alpha-1	1.42
Caldesmon ***	1.41
Nuclear mitotic apparatus protein 1	1.39
40S ribosomal protein S3a	1.37
Peroxiredoxin-6	1.32
Coatomer subunit beta	1.32
Non-P'U domain-containing octamer-binding protein	1.32
GTP-binding nuclear protein Ran	1.31
Protein transport protein Sec31A	1.31
Catenin alpha-1 ***	1.30
Myosin-9	1.29
60S ribosomal protein L18a	1.29
Histidine--tRNA ligase, cytoplasmic	1.28
AP-2 complex subunit alpha-2	1.28
Nardilysin	1.27
60S ribosomal protein L23a	1.26
Leucine-rich repeat-containing protein 59	1.26
Translational activator GCN1	1.26
Programmed cell death 6-interacting protein	1.26
Fermitin family homolog 2 ***	1.26
26S proteasome non-ATPase regulatory subunit 2	1.26
Glucosamine--fructose-6-phosphate aminotransferase [isomerizing] 1 ***	1.25
Hypoxia up-regulated protein 1	1.24
60S acidic ribosomal protein P2	1.24
Integrin alpha-2	1.24
78 kDa glucose-regulated protein	1.23
Plastin-3 ***	1.23
Aminopeptidase N	1.22
Importin-5	1.22
Nestin	0.83
Long-chain-fatty-acid--CoA ligase 4	0.82
Microtubule-associated protein 4	0.82
Lamin-B2	0.81
Atlastin-3	0.81
Reticulocalbin-2	0.81
Neuroblast differentiation-associated protein AHNAK	0.81
LIM and SH3 domain protein 1	0.81
Ubiquitin carboxyl-terminal hydrolase 14	0.81
Galectin-1	0.80
Heterogeneous nuclear ribonucleoprotein D-like	0.80
Eukaryotic translation initiation factor 2 subunit 2	0.78
5'-nucleotidase	0.78
CD166 antigen ***	0.77
Low-density lipoprotein receptor	0.76
Xaa-Pro dipeptidase	0.76
Beta-hexosaminidase subunit beta	0.75
Chondroitin sulfate proteoglycan 4	0.75
Src substrate cortactin	0.74
Nuclease-sensitive element-binding protein 1 ***	0.74
Thioredoxin reductase 1, cytoplasmic	0.74
CD97 antigen	0.72
Yorkie homolog	0.67
Sequestosome-1	0.67
Glypican-1	0.66
Myristoylated alanine-rich C-kinase substrate ***	0.65
Calpastatin	0.64

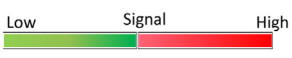

using decoy database), obtained from 14,097 distinct peptides and 28,303 total spectra (data not shown). To distinguish these and to generate a comprehensive list of proteins regulated by rhTGF-β1, a data processing pipeline was employed. Initially protein differential expression was measured as iTRAQ ratios between two groups of interest (*i.e.* rhTGF-β1 *vs.* none treated). Then, to be regarded as significant, proteins were required to be identified by at least two unique peptides and considered highly regulated (<0.83 for down-regulated proteins or >1.2 for up-regulated proteins).

Table 4
Proteomics analysis of HF19 upon PXS64 treatment A group of 20 proteins was found to be regulated by PXS64, with 11 proteins being a subset from the group of proteins up-regulated by rhTGF-β1.

Down-regulated by TGF-β1 + PXS64	
Fermitin family homolog 2	Also regulated by TGF-β1 alone
Elongation factor 2	
Fibronectin	
Collagen alpha-2(I) chain	
Tensin-1	
Collagen alpha-1(I) chain	
Collagen alpha-1(V) chain	
Thrombospondin-1	
CTGF	
Asparagine synthetase	
Leiomodin-1	
UDP-N-acetylhexosamine pyrophosphorylase	
S-adenosylmethionine synthase isoform type-2	

Up-regulated by TGF-β1 + PXS64	
Cadherin-6	Also regulated by TGF-β1 alone
Pre-B-cell leukemia transcription factor-interacting protein 1	
10 kDa heat shock protein mitochondrial	
Integrin alpha-2	
60 kDa heat shock protein mitochondrial	
N-acetylglucosamine-6-sulfatase	
Cathepsin D	

Upon rhTGF-β1 treatment, 55 and 82 proteins were found to be regulated in the HF19 and NHLF cell lines respectively (Tables 2 and 3), with a commonality in 18 proteins between HF19 and NHLF (proteins highlighted by the asterisk in Tables 2 and 3). The functional significance of the regulated proteins was evaluated by linking known proteins to their putative biological functions, based on their gene ontology annotations and their correlation in the Ingenuity Knowledge Base. The top canonical pathways regulated by rhTGF-β1 in HF19 cells were ILK signalling, tight junction signalling, hepatic fibrosis/hepatic stellate cell activation and caveolar-mediated endocytosis signalling. For NHLF cells, the regulated canonical pathways were eIF2, eIF4 and p70S6K signalling, hepatic fibrosis/hepatic stellate cell activation, RAN signalling and mTOR signalling.

HF19 cells treated with rhTGF-β1 concomitant with PXS64 showed a differential expression of 20 proteins (Table 4), none of which were apoptotic pathways. Interestingly 11 of these proteins were also a subset of the proteins regulated by rhTGF-β1. In the NHLF cells a group of 55 proteins were regulated by co-treatment with rhTGF-β1 + PXS64, with 38 being a subset regulated by rhTGF-β1 alone (Table 5). Remarkably, the majority of the proteins inhibited by PXS64 returned to baseline levels. It is important to note that none of the caspase family members or other apoptotic related proteins (such as calpain and BCL-1) were altered after treatment with PXS64. In addition, PXS64 was tested in a standard cell health assay [49] and concentrations of up to 100 μM showed no signs of toxicity (data not shown).

Table 5
Proteomics analysis of NHLF upon PXS64 treatment A group of 55 proteins was found to be regulated by PXS64, with 39 proteins being a subset from the group of proteins down regulated by rhTGF-β1. Data presented are from one experiment using single culture.

Down-regulated by TGF-β1 + PXS64	
Importin-5	Also regulated by TGF-β1 alone
Myosin-9	
Translational activator GCN1	
Transforming growth factor-beta-induced protein ig-h3	
Peroxiredoxin-6	
Nardilysin	
60S acidic ribosomal protein P2	
Ubiquitin-40S ribosomal protein S27a	
AP-2 complex subunit alpha-1	
Unconventional myosin-Ib	
Plastin-3	
60S ribosomal protein L7	
60S ribosomal protein L11	
Caldesmon	
Tenascin	
GTP-binding nuclear protein Ran	
40S ribosomal protein S10	
Collagen alpha-1(II) chain	
Fibronectin	
60S ribosomal protein L18a	
Plasminogen activator inhibitor 1 RNA-binding protein	
Alpha-actinin-1	
Probable ATP-dependent RNA helicase DDX17	
Collagen alpha-2(II) chain	
40S ribosomal protein S8	
Protein disulfide-isomerase	
A-kinase anchor protein 12	
Transgelin	
DNA mismatch repair protein Msh6	
Prelamin-A/C	
Plasminogen activator inhibitor 2	
Eukaryotic translation initiation factor 3 subunit A	
S-formylglutathione hydrolase	
40S ribosomal protein S11	
AP-3 complex subunit delta-1	
Serine/threonine-protein phosphatase 2A 65 kDa regulatory subunit A alpha isoform	
Cysteine--tRNA ligase, cytoplasmic	
DNA topoisomerase 2-alpha	
Importin subunit alpha-2	

Up-regulated by TGF-β1 + PXS64	
Matrix metalloproteinase-14	Also regulated by TGF-β1 alone
Paired amphipathic helix protein Sin3b	
Calpastatin	
V-type proton ATPase subunit B, brain isoform	
Reticulon-4	
Xaa-Pro dipeptidase	
Long-chain-fatty-acid--CoA ligase 4	
Thioredoxin reductase 1, cytoplasmic	
Atlastin-3	
Tissue factor pathway inhibitor 2	
Peptidyl-prolyl cis-trans isomerase FKBP4	
Heat shock 70 kDa protein 4L	
Cytoplasmic dynein 1 intermediate chain 2	
AP-1 complex subunit gamma-1	
Pyruvate kinase isozymes M1/M2	
Long-chain-fatty-acid--CoA ligase 3	

4. Discussion

The present study demonstrates that the lipophilic mannose-6-phosphate (M6P) analogue, PXS64, dampens rhTGF-β1-induced collagen, fibronectin and αSMA production by NHLF and HF19 fibroblasts. In addition, PXS64 is a strong inhibitor of fibrotic genes in IPF patient fibroblasts. Proteomics analysis confirmed that the action of PXS64 was specific to the TGF-β1 pathway.

Fibroblast migration, proliferation and transdifferentiation are present in normal lungs and the transformation into a myofibroblast-like cell type is regarded as an early step in the fibrotic process [50,51]. Myofibroblast recruitment and differentiation in the lung enhances scarring and fibrosis, resulting in pulmonary stiffness and impairment of lung function [12,50,52].

In vitro fibroblast-to-myofibroblast transdifferentiation has been shown to be induced by TGF-β1 [53], thus it was not unexpected that stimulation of NHLF and HF19 cells with active rhTGF-β1 would induce this process. However, there were distinct differences in the response of these fibroblasts, with both cells showing increases in collagen and fibronectin but only HF19 (and not NHLF cells) highly expressing αSMA. This was further confirmed by proteomics analysis in which rhTGF-β1 regulated a number of different proteins in HF19 compared to NHLF cells. Overall the protein expression results served to confirm that both NHLF and HF19 are responsive to rhTGF-β1 and underwent differentiation. The underlying mechanistic differences in protein synthesis of NHLF and HF19

were not elucidated in this study. However, the dissimilarities could be indicative of a delay in activating certain pathways, which might be attributed to the origin of the fibroblasts, or simply due to the fact that that NHLF are primary cells and HF19 are an immortalised cell line. In fact, a number of reports have indicated inherent dissimilarities between primary and immortalised cells [54–56].

Idiopathic pulmonary fibrosis is a condition for which there is no effective therapy to restore structural and/or functional normality. As such, the prevention of lung scarring from excessive fibroblast-to-myofibroblast transdifferentiation would be of great clinical relevance. An interesting approach is the use of M6P or the analogue PXS25, as they have shown great promise in variety of inflammation and fibrosis models [18,20–22,24–27]. In the current study, the lipophilic M6P analogue PXS64 was investigated during rhTGF-β1 induced myofibroblast differentiation. Treatment with PXS64 prevented induction of fibrotic proteins and mRNA in all cell types tested. Even when fibroblasts were no longer in contact with the compound (for over 12 h) anti-fibrotic effects were still observable, indicating a lasting effect mediated only by a transitory exposure to the compound. Surprisingly, the treatment was found to reverse the effects of rhTGF-β1, indicating that PXS64 does not impede cell activation or priming, but rather reduces TGF-β1 downstream signalling.

To date a number of studies have indicated that cellular density can alter the surrounding environment by influencing cellular phenotype and consequently susceptibility to therapeutic intervention. As shown by Masur et al., fibroblasts seeded at low density produce a myofibroblast population of >70%; however, when seeded at high density the fibroblasts produced cultures with only 5–10% myofibroblasts [41]. Furthermore, Petridou et al. showed that the low density cultures expressed more αSMA than high density cultures [42]. Later studies have also shown that cell density can influence the mechanical properties of cells [43], with high cellular density proposed be sufficient to induce quiescence [44,45]. In the subconfluent fibroblast culture system, PXS64 demonstrated exceptional anti-fibrotic activity, equal to that displayed by Pirfenidone. While in the high fibroblast confluency model, PXS64 maintained its anti-fibrotic effects whereas Pirfenidone completely lost efficacy. Taken together, the results suggest that PXS64 inhibits fibrotic protein expression independent of the speed at which myofibroblasts are differentiating or the status of cellular quiescence.

Whilst the exact mode of action of PXS64 was not determined, the findings from this study provide important clues as to what may be occurring. The action of M6P itself has proven controversial as it was originally proposed to occur *via* its membrane bound receptor (cation independent mannose-6-phosphate receptor/CIMPR) [17,57] however more recent studies have described otherwise [23,58]. Wong et al. demonstrated that TGF-β1 activation in corneal fibroblasts was M6P independent [23], while Barnes et al. showed no evidence of CIMPR in M6P treated tissue [58]. Nevertheless, it was important to address whether M6P and its analogues could block the binding of latent TGF-β binding to CIMPR, inhibit its activation and, consequently, any downstream signalling events in fibroblasts. Notably, in the cellular model used in this study, active rhTGF-β1 was added directly to the fibroblasts, thereby circumventing the latent TGF-β/CIMPR interaction and consequently indicating that the inhibitory effect of PXS64 was not, in actual fact, dependent on CIMPR. In addition, in both CIMPR-negative fibroblasts as well as CIMPR-negative fibroblasts ectopically expressing human CIMPR, PXS64 inhibited TGF-β1 induced fibronectin expression. Based on these observations, CIMPR does not appear to have any contribution to the pathways blocked by PXS64.

It is noteworthy that whilst the lipophilic M6P analogue PXS64 strongly inhibited TGF-β1-induced fibronectin expression, M6P nor the more polar M6P analogue PXS25 had an effect. These results are in contrast to what has been previously described, whereby M6P and PXS25 were shown to effectively inhibit disease models [18,20–22,24–27]. Although we currently cannot fully explain these observations, a possibility could be due to variances in cell lines, activation pathways and differences in cell membrane permeability. It is also plausible that given the high lipophilicity of PXS64 (a prodrug of PXS25) it diffused across the cell membrane and, once within the intracellular space, hydrolysed into PXS25. As such the prolonged effect exhibited by PXS64 may, in actual fact, be due to the intracellular presence of PXS25. In contrast, M6P and PXS25 are not highly permeable and thus any intracellular concentrations would potentially have been too low to demonstrate an effect.

Having ruled out CIMPR as a putative target of PXS64, protein analysis of NHLF and HF19 cells upon active rhTGF-β1 treatment was established in an attempt to identify the pathways/signalling events involved in the mode of action. Although there were clear phenotypical differences between these fibroblasts, PXS64 successfully inhibited fibrotic markers suggestive of the specific action of PXS64 on the TGF-β1 pathway. Proteins of special interest for the biology of fibrosis included thrombospondin-1, plasminogen activator inhibitor 1, fibronectin, collagen alpha-1(I) chain, collagen alpha-2(I) chain, transforming growth factor-beta-induced protein ig-h3, fermitin family homolog 2, procollagen-lysine, 2-oxoglutarate 5-dioxygenase 2, tenascin, plastin-3, caldesmon, catenin alpha-1, prolyl 4-hydroxylase subunit alpha-2 [59–67]. These results are in agreement with the hypothesis that TGF-β1 promotes the synthesis of proteins which are critical to lung fibrosis. The other proteins were in the metabolic pathway, consistent with the proliferative effect of TGF-β1 [13,37]. It is noteworthy that a subset of the proteins (transgelin, moesin, thioredoxin, electron-transfer flavoprotein alpha-subunit, mitochondrial precursor, NAD(P)H dehydrogenase [quinone] and nuclease sensitive element binding protein) were also identified as part of the protein expression of A549 human lung adenocarcinoma stimulated with TGF-β [68], indicative of a common downstream process of these cells. As is evident from the changes in cell morphology, TGF-β1 mediated cytoskeletal reorganisation. These changes in the cytoskeleton play a central role in the regulation of cellular processes linked to anchorage, cell growth and cell migration [62,69,70]. Of the up-regulated proteins, integrin alpha, myosin, collagen and fibronectin regulate cytoskeletal reorganisation. These proteins are also implicated in the dynamic process of cellular motility and/or the interaction of cells with the extracellular matrix. Specifically in the case of the up-regulated protein collagen, it is recognised that its accumulation is a major feature of pulmonary fibrosis and other fibrotic lesions [62]. Interestingly PXS64 was able to dampen these proteins, in addition to inhibiting thrombospondin, CTGF, elongation factor 2 and tensin, fermintin family homolog, all proteins associated with some form of fibrosis, indicative of the anti-fibrotic role of PXS64. The biological network analysis using the Ingenuity pathway tool provided information to link known proteins to putative biological processes through review of the literature. This path network analysis further strengthens the data interpretation by identifying known regulatory molecules of TGF-β1, like ILK signalling, tight junction, RAN and mTOR signalling.

Taken together, these results show the anti-fibrotic effects of PXS64 and highlight the potential of a lipophilic M6P analogue as a potential therapeutic tool, in addition to being a novel approach to dissect the mechanisms underlying fibrosis.

Disclosures

H. Schilter, A. D. Findlay, M. Deodhar and W. Jarolimek are employees of Pharmaxis, a for profit organisation with ownership of PXS64, which is the compound described in the paper. In addition,

V. Leksa, A. Ohradanova-Repic, H. Stockinger, X. Song, M. Molloy performed experiments with financial support provided by Pharmaxis.

Acknowledgements

Lily Guo for experimental support. Kara Batte (Ohio State University, Marsh lab) for the help and contribution with IPF cell RNA extraction and qRT–PCR. Natasha Care (Australian Proteome Analysis Facility) for the contribution with the iTRAQ experiments and Dana Pascovici (Australian Proteome Analysis Facility) for the iTRAQ statistical analysis. This work was supported by the FWF–Austrian Science Fund (P22908) and VEGA – Slovak Grant Agency (2/0063/14) grants to Vladimir Leksa and also supported by the National Institutes of Health under award numbers R01HL102464 and RO1HL109481.

References

[1] T.R. Cox, J.T. Erler, Remodeling and homeostasis of the extracellular matrix: implications for fibrotic diseases and cancer, Dis. Model. Mech. 4 (2011) 165–178.
[2] K. Borensztajn, J. Stiekema, S. Nijmeijer, P.H. Reitsma, M.P. Peppelenbosch, C.A. Spek, Factor xa stimulates proinflammatory and profibrotic responses in fibroblasts via protease-activated receptor-2 activation, Am. J. Pathol. 172 (2008) 309–320.
[3] M. Selman, V.J. Thannickal, A. Pardo, D.A. Zisman, F.J. Martinez, J.P. Lynch 3rd, Idiopathic pulmonary fibrosis: pathogenesis and therapeutic approaches, Drugs 64 (2004) 405–430.
[4] A. Ghahary, E.E. Tredget, A. Ghahary, M.A. Bahar, C. Telasky, Cell proliferating effect of latent transforming growth factor-beta1 is cell membrane dependent, Wound Repair Regen. 10 (2002) 328–335.
[5] R. Gillitzer, M. Goebeler, Chemokines in cutaneous wound healing, J. Leukoc. Biol. 69 (2001) 513–521.
[6] H. Ihn, The role of TGF-beta signaling in the pathogenesis of fibrosis in scleroderma, Arch. Immunol. Ther. Exp. (Warsz) 50 (2002) 325–331.
[7] G.G. Gauglitz, H.C. Korting, T. Pavicic, T. Ruzicka, M.G. Jeschke, Hypertrophic scarring and keloids: pathomechanisms and current and emerging treatment strategies, Mol. Med. 17 (2011) 113–125.
[8] J.W. Penn, A.O. Grobbelaar, K.J. Rolfe, The role of the TGF-beta family in wound healing, burns and scarring: a review, Int. J. Burns. Trauma. 2 (2012) 18–28.
[9] A.L. Tatler, G. Jenkins, TGF-beta activation and lung fibrosis, Proc. Am. Thorac. Soc. 9 (2012) 130–136.
[10] O. Lepparanta, C. Sens, K. Salmenkivi, V.L. Kinnula, J. Keski-Oja, M. Myllarniemi, K. Koli, Regulation of TGF-beta storage and activation in the human idiopathic pulmonary fibrosis lung, Cell Tissue Res. 348 (2012) 491–503.
[11] A.C. Midgley, M. Rogers, M.B. Hallett, A. Clayton, T. Bowen, A.O. Phillips, R. Steadman, Transforming growth factor-beta1 (TGF-beta1)-stimulated fibroblast to myofibroblast differentiation is mediated by hyaluronan (HA)-facilitated epidermal growth factor receptor (EGFR) and CD44 co-localization in lipid rafts, J. Biol. Chem. 288 (2013) 14824–14838.
[12] A. Leask, D.J. Abraham, TGF-beta signaling and the fibrotic response, FASEB J. 18 (2004) 816–827.
[13] F. Strutz, M. Zeisberg, A. Renziehausen, B. Raschke, V. Becker, C. van Kooten, G. Muller, TGF-beta 1 induces proliferation in human renal fibroblasts via induction of basic fibroblast growth factor (FGF-2), Kidney Int. 59 (2001) 579–592.
[14] W.T. Harris, D.R. Kelly, Y. Zhou, D. Wang, M. Macewen, J.S. Hagood, J.P. Clancy, N. Ambalavanan, E.J. Sorscher, Correction Myofibroblast differentiation and enhanced TGF-b signaling in cystic fibrosis lung disease, PLOS ONE (2013) 8.
[15] T. Wyss-Coray, P. Borrow, M.J. Brooker, L. Mucke, Astroglial overproduction of TGF-beta 1 enhances inflammatory central nervous system disease in transgenic mice, J. Neuroimmunol. 77 (1997) 45–50.
[16] T.L. Yeung, C.S. Leung, K.K. Wong, G. Samimi, M.S. Thompson, J. Liu, T.M. Zaid, S. Ghosh, M.J. Birrer, S.C. Mok, TGF-beta modulates ovarian cancer invasion by upregulating CAF-derived versican in the tumor microenvironment, Cancer Res. 73 (2013) 5016–5028.
[17] S.J. Bates, E. Morrow, A.Y. Zhang, H. Pham, M.T. Longaker, J. Chang, Mannose-6-phosphate, an inhibitor of transforming growth factor-beta, improves range of motion after flexor tendon repair, J. Bone Joint Surg. Am. 88 (2006) 2465–2472.
[18] D.A. Black, M. Tucci, A. Puckett, H. Benghuzzi, Histopathological and biomechanical parameters of repaired rat achilles tendons treated with and without mannose-6-phosphate, Biomed. Sci. Instrum. 48 (2012) 43–48.
[19] C. Xia, X.Y. Yang, Y. Wang, S. Tian, Inhibition effect of mannose-6-phosphate on expression of transforming growth factor beta receptor in flexor tendon cells, Orthopedics 34 (2011) 21.
[20] W.C. Ngeow, S. Atkins, C.R. Morgan, A.D. Metcalfe, F.M. Boissonade, A.R. Loescher, P.P. Robinson, Histomorphometric changes in repaired mouse sciatic nerves are unaffected by the application of a scar-reducing agent, J. Anat. 219 (2011) 638–645.
[21] W.C. Ngeow, S. Atkins, C.R. Morgan, A.D. Metcalfe, F.M. Boissonade, A.R. Loescher, P.P. Robinson, The effect of mannose-6-phosphate on recovery after sciatic nerve repair, Brain Res. 1394 (2011) 40–48.
[22] W.C. Ngeow, S. Atkins, C.R. Morgan, A.D. Metcalfe, F.M. Boissonade, A.R. Loescher, P.P. Robinson, A comparison between the effects of three potential scar-reducing agents applied at a site of sciatic nerve repair, Neuroscience 181 (2011) 271–277.
[23] J.K. Wong, A.D. Metcalfe, R. Wong, J. Bush, C. Platt, A. Garcon, N. Goldspink, D.A. McGrouther, M.W. Ferguson, Reduction of tendon adhesions following administration of Adaprev, a hypertonic solution of mannose-6-phosphate: mechanism of action studies, PLOS ONE 9 (2014) e112672.
[24] D.O. Willenborg, C.R. Parish, W.B. Cowden, Phosphosugars are potent inhibitors of central nervous system inflammation, FASEB J. 3 (1989) 1968–1971.
[25] D.O. Willenborg, C.R. Parish, W.B. Cowden, Inhibition of adjuvant arthritis in the rat by phosphosugars and the alpha-glucosidase inhibitor castanospermine, Immunol. Cell Biol. 70 (Pt 6) (1992) 369–377.
[26] M.R. Bartlett, H.S. Warren, W.B. Cowden, C.R. Parish, Effects of the anti-inflammatory compounds castanospermine, mannose-6-phosphate and fucoidan on allograft rejection and elicited peritoneal exudates, Immunol. Cell Biol. 72 (1994) 367–374.
[27] M.G. Wong, U. Panchapakesan, W. Qi, D.G. Silva, X.M. Chen, C.A. Pollock, Cation-independent mannose 6-phosphate receptor inhibitor (PXS25) inhibits fibrosis in human proximal tubular cells by inhibiting conversion of latent to active TGF-beta1, Am. J. Physiol. Renal Physiol. 301 (2011) F84–F93.
[28] K. Vuorinen, F. Gao, T.D. Oury, V.L. Kinnula, M. Myllarniemi, Imatinib mesylate inhibits fibrogenesis in asbestos-induced interstitial pneumonia, Exp. Lung Res. 33 (2007) 357–373.
[29] Z.Q. Wang, M.R. Fung, D.P. Barlow, E.F. Wagner, Regulation of embryonic growth and lysosomal targeting by the imprinted IGF2/MPR gene, Nature 372 (1994) 464–467.
[30] V. Leksa, S. Godar, M. Cebecauer, I. Hilgert, J. Breuss, U.H. Weidle, V. Horejsi, B.R. Binder, H. Stockinger, The n terminus of mannose 6-phosphate/insulin-like growth factor 2 receptor in regulation of fibrinolysis and cell migration, J. Biol. Chem. 277 (2002) 40575–40582.
[31] D. Pascovici, D.M. Gardiner, X. Song, E. Breen, P.S. Solomon, T. Keighley, M.P. Molloy, Coverage and consistency: bioinformatics aspects of the analysis of multirun iTRAQ experiments with wheat leaves, J. Proteome Res. 12 (2013) 4870–4881.
[32] X. Song, J. Bandow, J. Sherman, J.D. Baker, P.W. Brown, M.T. McDowell, M.P. Molloy, Itraq experimental design for plasma biomarker discovery, J. Proteome Res. 7 (2008) 2952–2958.
[33] K. Minton, Extracellular matrix: preconditioning the ECM for fibrosis, Nat. Rev. Mol. Cell Biol. 15 (2014) 766–767.
[34] N.J. Kenyon, R.W. Ward, G. McGrew, J.A. Last, TGF-beta1 causes airway fibrosis and increased collagen I and III mRNA in mice, Thorax 58 (2003) 772–777.
[35] U. Kucich, J.C. Rosenbloom, G. Shen, W.R. Abrams, A.D. Hamilton, S.M. Sebti, J. Rosenbloom, TGF-beta1 stimulation of fibronectin transcription in cultured human lung fibroblasts requires active geranylgeranyl transferase I, phosphatidylcholine-specific phospholipase C, protein kinase C-delta, and p38, but not erk1/erk2, Arch. Biochem. Biophys. 374 (2000) 313–324.
[36] D. Kurosaka, Y. Muraki, M. Inoue, H. Katsura, TGF-beta 2 increases alpha-smooth muscle actin expression in bovine retinal pigment epithelial cells, Curr. Eye Res. 15 (1996) 1144–1147.
[37] G. Chen, N. Khalil, TGF-beta1 increases proliferation of airway smooth muscle cells by phosphorylation of map kinases, Respir. Res. 7 (2006) 2.
[38] Q. Xu, J.T. Norman, S. Shrivastav, J. Lucio-Cazana, J.B. Kopp, In vitro models of TGF-beta-induced fibrosis suitable for high-throughput screening of antifibrotic agents, Am. J. Physiol. Renal Physiol. 293 (2007) F631–F640.
[39] A. Bergeron, P. Soler, M. Kambouchner, P. Loiseau, B. Milleron, D. Valeyre, A.J. Hance, A. Tazi, Cytokine profiles in idiopathic pulmonary fibrosis suggest an important role for TGF-beta and IL-10, Eur. Respir. J. 22 (2003) 69–76.
[40] M.C. Emblom-Callahan, M.K. Chhina, O.A. Shlobin, S. Ahmad, E.S. Reese, E.P. Iyer, D.N. Cox, R. Brenner, N.A. Burton, G.M. Grant, S.D. Nathan, Genomic phenotype of non-cultured pulmonary fibroblasts in idiopathic pulmonary fibrosis, Genomics 96 (2010) 134–145.
[41] S.K. Masur, H.S. Dewal, T.T. Dinh, I. Erenburg, S. Petridou, Myofibroblasts differentiate from fibroblasts when plated at low density, Proc. Natl. Acad. Sci. U. S. A. 93 (1996) 4219–4223.
[42] S. Petridou, O. Maltseva, S. Spanakis, S.K. Masur, TGF-beta receptor expression and smad2 localization are cell density dependent in fibroblasts, Invest. Ophthalmol. Vis. Sci. 41 (2000) 89–95.
[43] R.I. Issa, B. Engebretson, L. Rustom, P.S. McFetridge, V.I. Sikavitsas, The effect of cell seeding density on the cellular and mechanical properties of a mechanostimulated tissue-engineered tendon, Tissue Eng. Part A 17 (2011) 1479–1487.
[44] J.J. Volwerk, G.B. Birrell, K.K. Hedberg, O.H. Griffith, A high level of cell surface phosphatidylinositol-specific phospholipase C activity is characteristic of growth-arrested 3T3 fibroblasts but not of transformed variants, J. Cell. Physiol. 151 (1992) 613–622.
[45] J. Pelisek, S. Armeanu, S. Nikol, Quiescence, cell viability, apoptosis and necrosis of smooth muscle cells using different growth inhibitors, Cell Prolif. 34 (2001) 305–320.
[46] A. Ghahary, E.E. Tredget, Q. Shen, Insulin-like growth factor-II/mannose 6 phosphate receptors facilitate the matrix effects of latent transforming growth factor-beta1 released from genetically modified keratinocytes in a fibroblast/keratinocyte co-culture system, J. Cell. Physiol. 180 (1999) 61–70.

[47] P.A. Dennis, D.B. Rifkin, Cellular activation of latent transforming growth factor beta requires binding to the cation-independent mannose 6-phosphate/insulin-like growth factor type II receptor, Proc. Natl. Acad. Sci. U. S. A. 88 (1991) 580–584.
[48] V. Leksa, S. Godar, H.B. Schiller, E. Fuertbauer, A. Muhammad, K. Slezakova, V. Horejsi, P. Steinlein, U.H. Weidle, B.R. Binder, H. Stockinger, TGF-beta-induced apoptosis in endothelial cells mediated by M6P/IGFII-R and mini-plasminogen, J. Cell Sci. 118 (2005) 4577–4586.
[49] J.K. Morelli, M. Buehrle, F. Pognan, L.R. Barone, W. Fieles, P.J. Ciaccio, Validation of an in vitro screen for phospholipidosis using a high-content biology platform, Cell Biol. Toxicol. 22 (2006) 15–27.
[50] W.T. Harris, D.R. Kelly, Y. Zhou, D. Wang, M. Macewen, J.S. Hagood, J.P. Clancy, N. Ambalavanan, E.J. Sorscher, Myofibroblast differentiation and enhanced TGF-B signaling in cystic fibrosis lung disease, PLOS ONE 8 (2013) e70196.
[51] R. Kalluri, E.G. Neilson, Epithelial-mesenchymal transition and its implications for fibrosis, J. Clin. Invest. 112 (2003) 1776–1784.
[52] N. Sakai, A.M. Tager, Fibrosis of two: epithelial cell-fibroblast interactions in pulmonary fibrosis, Biochim. Biophys. Acta 1832 (2013) 911–921.
[53] T. Meyer-Ter-Vehn, B. Katzenberger, H. Han, F. Grehn, G. Schlunck, Lovastatin inhibits TGF-beta-induced myofibroblast transdifferentiation in human tenon fibroblasts, Invest. Ophthalmol. Vis. Sci. 49 (2008) 3955–3960.
[54] E.A. Lidington, D.L. Moyes, A.M. McCormack, M.L. Rose, A comparison of primary endothelial cells and endothelial cell lines for studies of immune interactions, Transpl. Immunol. 7 (1999) 239–246.
[55] H. Kim, S. You, L.K. Foster, J. Farris, D.N. Foster, The rapid destabilization of p53 mRNA in immortal chicken embryo fibroblast cells, Oncogene 20 (2001) 5118–5123.
[56] S. Tommasi, A. Zheng, A. Weninger, S.E. Bates, X.A. Li, X. Wu, M. Hollstein, A. Besaratinia, Mammalian cells acquire epigenetic hallmarks of human cancer during immortalization, Nucleic Acids Res. 41 (2013) 182–195.
[57] N.M. Dahms, L.J. Olson, J.J. Kim, Strategies for carbohydrate recognition by the mannose 6-phosphate receptors, Glycobiology 18 (2008) 664–678.
[58] J. Barnes, D. Warejcka, J. Simpliciano, S. Twining, R. Steet, Latency-associated peptide of transforming growth factor-beta1 is not subject to physiological mannose phosphorylation, J. Biol. Chem. 287 (2012) 7526–7534.
[59] M.T. Sweetwyne, J.E. Murphy-Ullrich, Thrombospondin1 in tissue repair and fibrosis: TGF-beta-dependent and independent mechanisms, Matrix Biol. 31 (2012) 178–186.
[60] A.K. Ghosh, D.E. Vaughan, PAI-1 in tissue fibrosis, J. Cell. Physiol. 227 (2012) 493–507.
[61] C. Kuhn, J.A. McDonald, The roles of the myofibroblast in idiopathic pulmonary fibrosis. Ultrastructural and immunohistochemical features of sites of active extracellular matrix synthesis, Am. J. Pathol. 138 (1991) 1257–1265.
[62] G. Raghu, S. Masta, D. Meyers, A.S. Narayanan, Collagen synthesis by normal and fibrotic human lung fibroblasts and the effect of transforming growth factor-beta, Am. Rev. Respir. Dis. 140 (1989) 95–100.
[63] N. Thapa, B.H. Lee, I.S. Kim, TGFBIp/betaig-h3 protein: a versatile matrix molecule induced by TGF-beta, Int. J. Biochem. Cell Biol. 39 (2007) 2183–2194.
[64] H. Qu, Y. Tu, X. Shi, H. Larjava, M.A. Saleem, S.J. Shattil, K. Fukuda, J. Qin, M. Kretzler, C. Wu, Kindlin-2 regulates podocyte adhesion and fibronectin matrix deposition through interactions with phosphoinositides and integrins, J. Cell Sci. 124 (2011) 879–891.
[65] A.J. van der Slot, E.A. van Dura, E.C. de Wit, J. De Groot, T.W. Huizinga, R.A. Bank, A.M. Zuurmond, Elevated formation of pyridinoline cross-links by profibrotic cytokines is associated with enhanced lysyl hydroxylase 2b levels, Biochim. Biophys. Acta 1741 (2005) 95–102.
[66] Y. Zhao, S.L. Young, J.C. McIntosh, Induction of tenascin in rat lungs undergoing bleomycin-induced pulmonary fibrosis, Am. J. Physiol. 274 (1998) L1049–L1057.
[67] Y. Ando, T. Moriyama, K. Oka, K. Takatsuji, M. Miyazaki, Y. Akagi, N. Kawada, Y. Isaka, M. Izumi, K. Yokoyama, A. Yamauchi, M. Horio, A. Ando, N. Ueda, K. Sobue, E. Imai, M. Hori, Enhanced interstitial expression of caldesmon in IgA nephropathy and its suppression by glucocorticoid-heparin therapy, Nephrol. Dial. Transplant. 14 (1999) 1408–1417 (Official publication of the European Dialysis and Transplant Association – European Renal Association).
[68] V.G. Keshamouni, G. Michailidis, C.S. Grasso, S. Anthwal, J.R. Strahler, A. Walker, D.A. Arenberg, R.C. Reddy, S. Akulapalli, V.J. Thannickal, T.J. Standiford, P.C. Andrews, G.S. Omenn, Differential protein expression profiling by iTRAQ-2DLC-MS/MS of lung cancer cells undergoing epithelial-mesenchymal transition reveals a migratory/invasive phenotype, J. Proteome Res. 5 (2006) 1143–1154.
[69] A. Huttenlocher, M.H. Ginsberg, A.F. Horwitz, Modulation of cell migration by integrin-mediated cytoskeletal linkages and ligand-binding affinity, J. Cell Biol. 134 (1996) 1551–1562.
[70] S. Cai, L. Pestic-Dragovich, M.E. O'Donnell, N. Wang, D. Ingber, E. Elson, P. De Lanerolle, Regulation of cytoskeletal mechanics and cell growth by myosin light chain phosphorylation, Am. J. Physiol. 275 (1998) C1349–C1356.